Advancement in Various Stages of Palm Oil Mill Effluent (POME) Treatment Process

Sabeeha N. B. A. Khadaroo, Phaik Eong Poh, Darwin Gouwanda, and Hui Min Tan

Abstract Palm oil milling has progressed over the years with modernization and technology development. However, treatment methods for palm oil mill effluent (POME) remain archaic with little improvement in technology; due to the inherent challenges associated with the characteristics of POME along with microbial population sensitive to operational changes in the existing treatment process. It is imperative for the resolutions taken in order to advance POME treatment to fulfill the 3'E's criteria—Efficient, Ease of operability, and Economic feasibility. This chapter presents an overview of three established methods that were tested at laboratory scale to modernize POME treatment—(i) implementing artificial intelligence for POME treatment; (ii) thermal pretreatment of POME coupled with dewatering device and (iii) post-treatment of anaerobically treated POME with coagulant assisted microbubble flotation. These enhancements have proven to improve the treated effluent quality substantially and can be integrated into existing plants.

Keywords Palm oil mil effluent · Anaerobic digestion · Automation · Dewatering · Microbubble flotation · Artificial intelligence

1 Introduction

Palm oil milling is a proven and reliable process that has been advancing over the years with the mechanization and development of modern technology (Menon, 2011). The milling process has improved considerably from being labor-intensive to the utilization of modern equipment. Meanwhile, the approach for treating wastewater generated from the milling process, i.e., palm oil mill effluent (POME) has remained unchanged for the past decades. The opted treatment process for POME is simple to operate and has a low maintenance cost, primarily to conform to environmental regulations. Additionally, a lack of skilled labor prevents alterations to the POME treatment process. A typical POME treatment system uses a series of ponds capable

S. N. B. A. Khadaroo · P. E. Poh (✉) · D. Gouwanda · H. M. Tan
School of Engineering, Monash University Malaysia, Jalan Lagoon Selatan, 47500 Bandar Sunway, Selangor, Malaysia
e-mail: poh.phaik.eong@monash.edu

D. C. Y. Foo et al. (eds.), *Sustainable Technologies for the Oil Palm Industry*,
https://doi.org/10.1007/978-981-19-4847-3_11

of treating POME to meet effluent discharge standards stipulated by authorities. Nevertheless, there are impediments associated with the implementation of ponding systems explicitly, which include (i) long treatment duration; (ii) low treatment efficiency; (iii) emission of odor and harmful greenhouse gases, and (iv) having a large footprint (Chin et al., 2013).

A vast range of new methods and technologies was proposed and developed to resolve the conundrums related to POME treatment. However, only a few of them have been adopted by the mills. In recent years, many new mills in Malaysia have implemented anaerobic digesters to replace the conventional anaerobic ponds in order to comply with the regulations for energy and environmental conservation. In short, ponding system is still the best alternative for POME treatment. Many new mills would choose to cover their ponds to capture greenhouse gas emissions from their open surfaces as it requires least work and investment. Question remains as how to convince the mill owners and other stakeholders to improve and even alter the existing POME treatment.

Considering the advantages and disadvantages of the ponding treatment system and the complications faced in the mill, solutions for advanced POME treatment should meet the 3'E's criteria:

i. **Efficient** and adaptive: This is essential due to the possibility of enforcing a stricter discharge standard in the future. The increasing demand for crude palm oil (CPO) also contributes to a higher generation of POME. Therefore, any new technologies should work efficiently and effectively in handling the augmented flow rate of POME.
ii. **Ease** of operation: Having a dearth of skilled workers entails that the POME treatment process should be relatively straightforward in its monitoring and operation. Any existing employees in the mill should be able to remedy process anomalies and problems to lessen productivity loss.
iii. **Economically** feasible: Many advances in wastewater treatment technology do not contemplate the economic feasibility in their implementation. Hence, they are always "good to have" instead of a "must have". It is advised that new advancements should take into account the implementation cost.

Two fundamental challenges in POME treatment are the high concentration of organic matter and erratic POME characteristics, which depend on many external factors. Anaerobic digestion is the primary treatment method used to eliminate most organic matter. However, the unpredictable characteristics of POME cause instability in the digestion process and the discrepancy in treated effluent quality. Moreover, the bacteria population for anaerobic digestion is problematic and susceptible to alterations in operating parameters. Therefore, treating POME anaerobically in a large pond for a prolonged time appeared practical to ensure the removal of contaminants from the wastewater. The large anaerobic pond allows equalization of POME and infers the minimum disruption to the consortium of bacteria present.

The ponds function at a moderately slow pace. POME is held in a single pond for 30 days. Hence, numerous ponds are needed to carry out the treatment process. With increased CPO production, more ponds are required to handle the higher generation

of POME, if the treatment duration is to be remained. Implementation of high-rate anaerobic digesters is more feasible, considering their shorter POME treatment duration, higher process proficiency, and the capability for biogas capture (Poh et al., 2020). The remaining question is that "How to convince mill owners that high-rate anaerobic digesters are the better option for POME treatment, given the inherent and operating challenges?" The above question can be addressed from two facets: (i) automated control of high-rate anaerobic digester using least instrumentations, and (ii) pre-treating POME prior to anaerobic digestion. Both are discussed in the following sub-sections.

2 Implementation of Artificial Intelligence (AI) in POME Treatment

Due to the many variables to be monitored in the wastewater treatment process, proper quality control and monitoring system are necessary. Implementing AI in the wastewater treatment process can provide several advantages. With the right configurations and minimal measured variables, AI can provide reasonably accurate estimation of the process characteristics in real-time. Knowing the possible results of a treatment process allows the operators to put preventive measures in place to counteract any undesired effect (Zhao et al., 2020). To demonstrate the feasibility of AI in treating POME, Tan et al. (2018b) used adaptive neural fuzzy interference to monitor and automate the high-rate anaerobic digester. Shocks were introduced to study its effect on the process and to further validate this method against the abrupt changes in POME. In the following sub-section, an experiment along with necessary process instrument control was set up to study how an adaptive neural fuzzy inference can enhance the treatment process of POME.

2.1 Automating an Up-Flow Anaerobic Sludge Blanket-Hollow Centered Packed Bed (UASB-HCPB) Reactor in POME Treatment

A laboratory-scale hybrid reactor, i.e., up-flow anaerobic sludge blanket-hollow centered packed bed (UASB-HCPB) was used in this study. The capacity of the reactor was 5L, while the inoculated seed sludge was taken as 10% of the operating volume of the reactor. The water bath was connected to the reactor to ensure the temperature of the reactor was set at 55 °C (Poh & Chong, 2014). A Prominent DF4a pump was fitted at the bottom of the reactor to feed diluted POME at the bottom of the reactor, and to augment the contact time between POME and inoculated seed sludge. This setup also ensures thorough mixing within the reactor. A water displacement column was mounted to measure the volume of biogas produced (Tan et al., 2018a).

The microcontroller selected for this study was Arduino Mega 2560. The flow rate of the Prominent DF4a pump was controlled by Arduino. An additional dosing pump (Prominent Solenoid Metering Pump) was utilized to add sodium bicarbonate to the wastewater if the reactor's pH dropped below 7.0. Several sensors were installed and connected to Arduino to measure several main characteristics of the POME. pH probes were used to monitor the pH of feed, reactor, and effluent online. A temperature probe was installed to monitor the temperature of mixed liquor within the reactor. Lastly, a methane sensor was mounted to detect the presence of methane in the biogas produced (Tan et al., 2018a). Figure 1 illustrates the process and instrumentation diagram of the above-described experimental setup.

2.2 *Adaptive Neuro-Fuzzy Inference System (ANFIS) for POME Anaerobic Digester*

The input and output variables chosen to build the ANFIS model for the UABS-HCPB reactor were pH, organic loading rate (OLR), chemical oxygen demand (COD), and the total suspended solids (TSS). These variables were selected since they provide information on the condition of the reactor. For instance, pH describes the reactor's physicochemical characteristics, while COD offers an insight into the biological properties and the efficiency of the reactor. These variables can be easily monitored using sensors, while the laboratory procedures to test these parameters are relatively simple. The mentioned parameters are also crucial in order for the wastewater to comply with the discharge standards (Tan et al., 2018b).

The reactor pH, temperature, COD, OLR, and biogas production were constantly monitored and controlled to ensure system's stability throughout the study. Closely monitoring of these parameters also offers several benefits: (1) It allows smooth operation and the detection of anomalies that could cause reactor failure; (2) It can reduce number of operators and tasks involved; (3) It can reduce sampling and testing frequency; and (4) It allows the operators to take preventive measures when an irregularity is detected. Table 1 lists the importance and actions taken for the parameters mentioned above to ensure the proper functioning of the reactor (Poh et al., 2020).

The simulation and modeling in this study were undertaken in the ANFIS editor available in MATLAB R2015b Fuzzy Logic Toolbox. A total of 282 days of data were collected and used in this study. The data were partitioned into two parts. The first part consists of 214 days of experimental data, which were used as the training set. The remaining part (68 days) was used for validation. The data were normalized using Eq. 1.

$$Y_{\text{norm}} = \frac{Y - Y_{\text{min}}}{Y_{\text{max}} - Y_{\text{min}}} \tag{1}$$

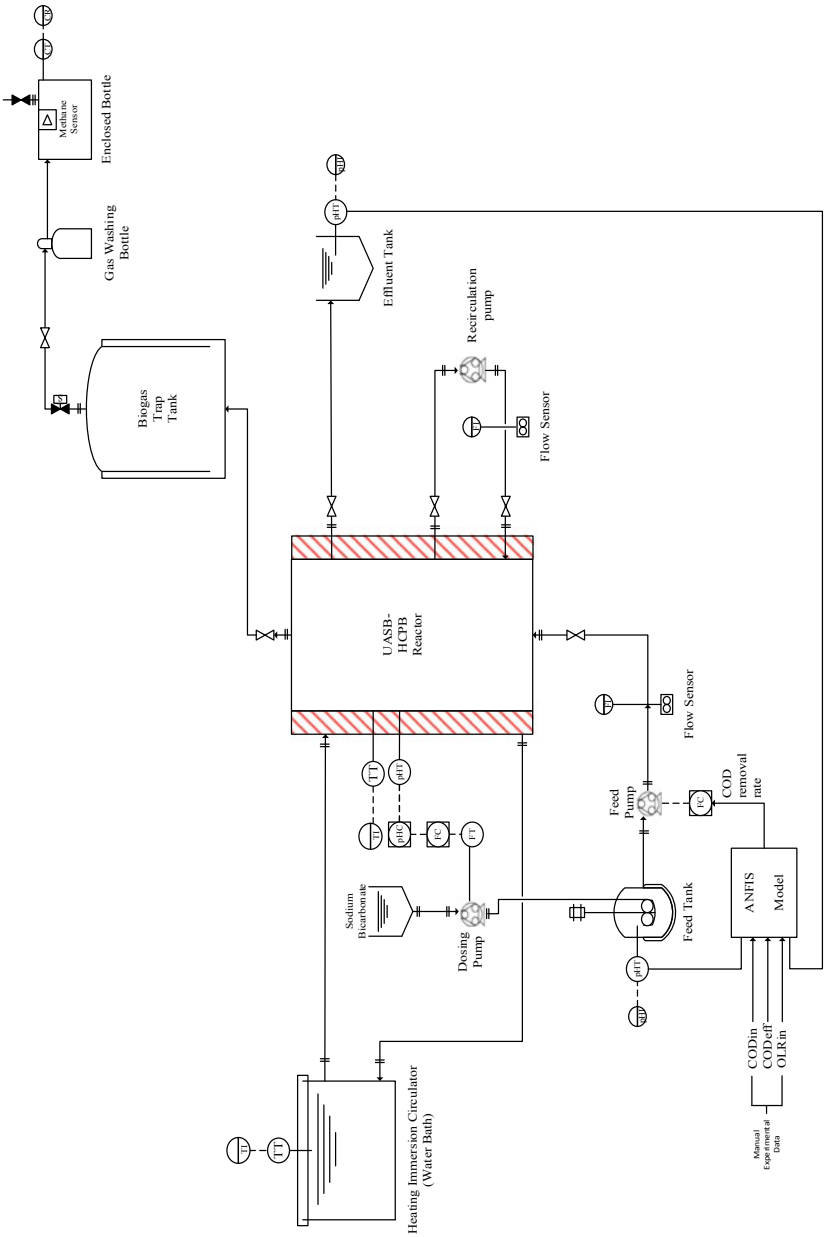

Fig. 1 Process and instrumentation diagram (P&ID) of the UASB-HCPB reactor after model implementation

Table 1 Parameters controlled and monitored in anaerobic digestion of POME

	Parameter	Importance	Countermeasures
Controlled parameters	pH	• Ensure digester balance • Provide ideal conditions for bacteria population	• Daily monitoring of feed, effluent, and reactor pH • Alkaline dosing
	OLR	• Biochemical reaction representation	• Daily measurement and monitoring • Included in ANFIS prediction
Monitored Parameters	COD	• Signifies efficacy of substrate utilization and metabolic activity • Dependent on influent flow rate and reactor working volume	• Removal efficiency is predicted using ANFIS, which allows corrective measures to be taken before reactor failure • Measurements (for feed and effluent) were conducted daily
	Biogas Quality	• Indicates performance of the reactor	• Real-time measurement daily using methane sensor to ensure biogas quality is maintained
	Temperature	• Provide ideal conditions for bacteria consortia • Ensure a high rate of reaction	• Daily monitoring at both water bath and within the reactor

where Y_{norm} is the normalized parameters, Y is the measured variables for the pH_{in}, COD_{in}, and OLR_{in}, Y_{max}, and Y_{min} are the maximum and minimum values of the variables.

The denormalization was performed using the same equation to compute the actual values of the predicted pH_{eff}, COD_{eff}, and TSS_{eff}.

Three fuzzy interference models designated as M1, M2, and M3 were built (Table 2). Each model was assigned distinct input and output parameters. Using four input parameters, M1 was constructed to predict the pH of the effluent (pH_{eff}). Meanwhile, using five and six input parameters, M2 and M3 were developed to predict the COD (COD_{eff}) and TSS of the effluent (TSS_{eff}), correspondingly. The effluent data was measured every 2 days since the reactor's hydraulic retention rate was set to two days. The effluent data measured 2 days prior ($t - 2$), known as historical data, were added to the models to enhance the prediction ability (Tan et al., 2018b).

Various measures were computed to assess the predictive ability of models M1, M2, and M3. These measure parameters were the average and standard deviations of the estimate errors, the determination coefficient denoted by R^2, the root mean square error denoted by RMSE, and the index of agreement denoted by IA. R^2, RMSE, and IA are parameters that indicate the discrepancy between the estimated and actual values. These parameters were evaluated using Eqs. 2, 3, and 4.

Table 2 ANFIS model setup

Model	Inputs	Output
M1	pH_{in}, COD_{in}, OLR_{in}, pH_{eff} (t − 2)	pH_{eff}
M2	pH_{in}, COD_{in}, OLR_{in}, pH_{eff} (t − 2), COD_{eff} (t − 2)	COD_{eff}
M3	pH_{in}, COD_{in}, OLR_{in}, pH_{eff} (t − 2), COD_{eff} (t − 2), TSS_{eff} (t − 2)	TSS_{eff}

$$R^2 = \frac{\left(\sum_{i=1}^{n}(A_i - A_m)(P_i - P_m)\right)^2}{\sum_{i=1}^{n}(A_i - A_m)^2 \sum_{i=1}^{n}(P_i - P_m)^2} \tag{2}$$

$$\text{RMSE} = \sqrt{\left(\frac{1}{n}\sum_{i=1}^{n}(P_i - A_i)^2\right)} \tag{3}$$

$$\text{IA} = 1 - \frac{\sum_{i=1}^{n}(P_i - A_i)^2}{\sum_{i=1}^{n}(|P_i - A_m| + |A_i - A_m|)^2} \tag{4}$$

where A represents actual measured values, P is the predicted values, m is the mean value, i is the initial value, and n is the number of data.

2.3 Results and Discussion

Table 3 presents the results obtained for the quantitative analysis to evaluate the performance of each model. Based on Table 3, M3 performed better as compared to M2 and M1 with the highest R^2, RMSE, and *IA* values. Meanwhile, Fig. 2 depicts the ability of M1 model in predicting the pH_{eff} values. Tan et al. (2018b) found that the average error and the standard deviation between the actual and predicted pH_{eff} were 2.06 and 1.68% congruently.

Albeit it can be observed that M1 was able to mimic the proclivity of the measured pH values, some incongruities were noted on days 10–14. The higher prediction of data was attributed to the drop in pH due to the decrease in alkalinity as the reactor was running at higher OLR of 36.32 kg COD/m^3day. However, this occurrence was not alarming since the alkalinity remained within a consistent range as the reactor

Table 3 ANFIS modeling results for anaerobic digestion of POME

Model	Input	Output	R^2	RMSE	IA
M1	pH_{in}, COD_{in}, OLR_{in}, pH_{eff} (t − 2)	pH_{eff}	0.63	0.0390	0.88
M2	pH_{in}, COD_{in}, OLR_{in}, pH_{eff} (t − 2), COD_{eff} (t − 2)	COD_{eff}	0.66	0.0618	0.89
M3	pH_{in}, COD_{in}, OLR_{in}, pH_{eff} (t − 2), COD_{eff} (t − 2), TSS_{eff} (t − 2)	TSS_{eff}	0.82	0.0377	0.95

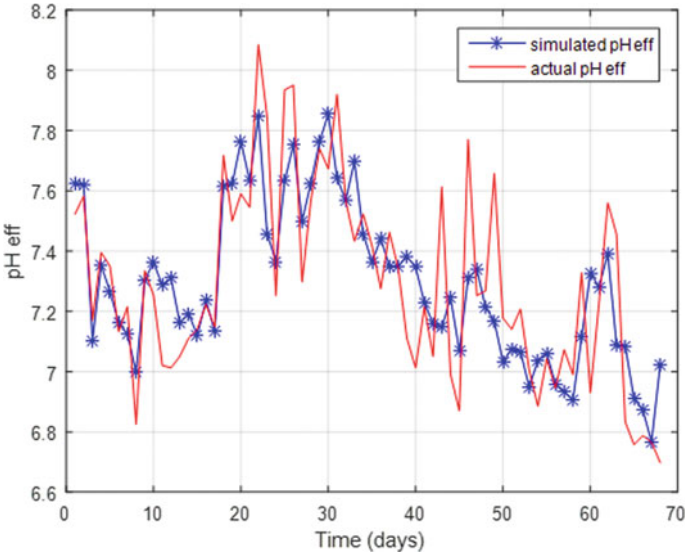

Fig. 2 Actual Effluent pH and simulated pH estimated by M1

achieved a steady state. Meanwhile, the disparities recorded on days 47–52 could be explained by the lag time taken for the bacteria consortium to adapt to the changes in pH. Since the reactor's optimum performance could not be attained instantly, the predicted pH_{eff} was lower than the actual values. The quantitative assessment in Table 3 shows that the R^2, RMSE, and IA values for the M1 model were computed to be 0.63, 0.0390, and 0.88, respectively.

On the other hand, the M2 model attained an average error and standard deviation of 8.32% and 7.65%, respectively. Albeit the average error and the standard deviation were greater than those in M1, due to the reactor's biological nature. The results achieved were considered satisfactory, and are in concurrence with studies conducted by (Hamawand & Baillie, 2015). Figure 3 depicts that M2 is relatively capable of providing compelling predictions, and can efficiently simulate the measured COD_{eff}. Moreover, it has the ability to forecast any unexpected spike in COD_{eff}, such as the one detected on day 18. In uncommon instances, it was observed that on day 8 and day 30, the model predicted almost consistent COD_{eff} for several consecutive days. A plausible explanation for this incident is ascribable to the variations in POME's physicochemical characteristics. (Poh et al., 2010) reported that low crop or high crop seasons considerably influence COD concentration, acidity, solid, as well as oil and grease contents of POME.

Additionally, the formation of a layer of scum was observed on day 8, which in turn caused an increase in the actual effluent values. Scum formation can decrease the reactor performance and make the modeling of the POME anaerobic digester difficult due to clogging in the pipes or solids washout from the bioreactor. The quantitative assessment for the M2 model was calculated to be 0.66 for the R^2, 0.0618 for the

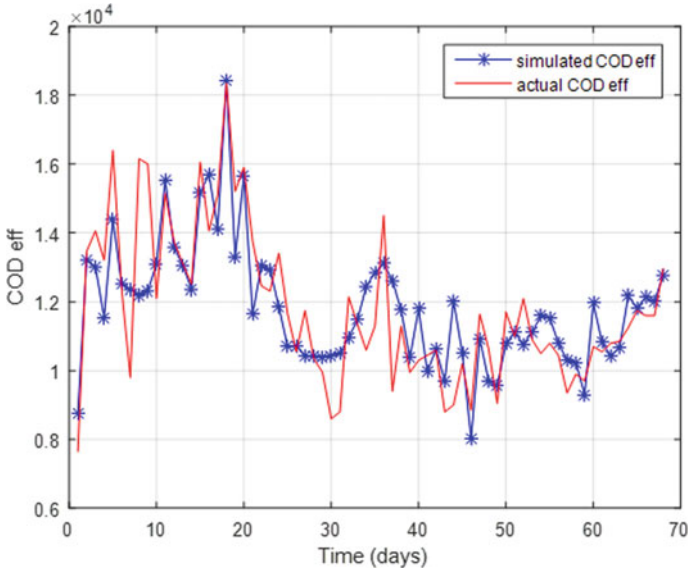

Fig. 3 Actual Effluent COD and simulated COD estimated by M2

RMSE, and 0.89 for the IA. Since the M1 and M2 models achieved R^2 and IA values at the lower side, the results indicate that M1 and M2 are capable of predicting the pH_{eff} and COD_{eff} correctly, nonetheless with a lack of precision.

Figure 4 demonstrates that M3 is able to predict the TSS_{eff} correctly with an average error and standard deviation of 6.93 and 6.28%, congruently. A more significant discrepancy was noted in M3 in comparison to M1. Meanwhile, it was noted that the deviation in M3 prediction was lower than in M2. This may occur due to the model's incapacity to predict the abrupt fall in TSS_{eff} on day 33, along with the sharp surge on day 37. These incidences are frequent in the anaerobic digester (Moreno, 2004; Murphy, 2007) and occur when POME concentration in the feed increases. A high concentration of POME triggers a higher OLR, which leads to larger particles flowing into the effluent tank.

Nonetheless, M3 can adequately predict TSS_{eff}, as shown in Fig. 4. M3 is also adept at simulating the abrupt rises and plunges, as illustrated on days 10–20. For quantitative analysis, M3 demonstrates superior prediction than M1 and M2 with R^2 of 0.82, and IA value of 0.95. The results achieved indicate that M3 has a superior prediction ability and higher accuracy than M1 and M2.

As theorized, the ANFIS model has the ability to predict the effluent's pH, COD and TSS accurately. The average errors computed ranged between 2.06 and 8.32%, while the standard deviation fluctuated between 1.38 and 7.65%. The trend predictions were deemed to be appropriate. The predicted tendencies were comparable to the measured data with minor variations. Moreover, the ANFIS model demonstrated

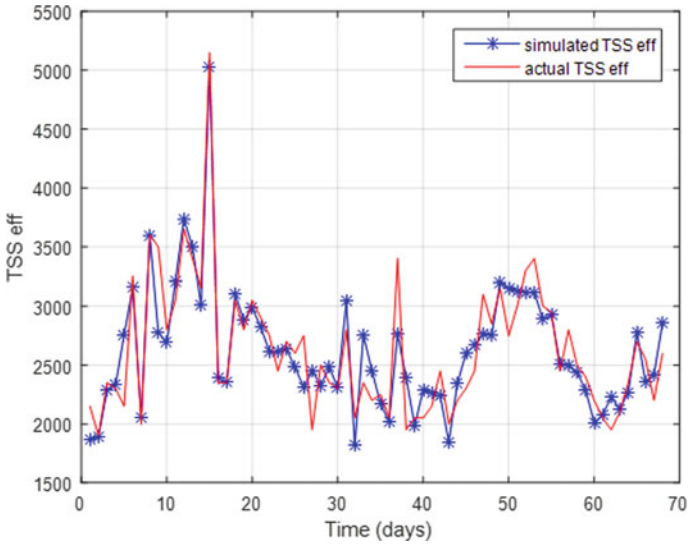

Fig. 4 Actual Effluent TSS and simulated TSS estimated by M3

the ability to manage unexpected fluctuations in the measured and predicted pH, COD, and TSS, as indicated by the results achieved.

3 Integration of Thermal Pretreatment and a Thickening Device

A lot of emphasis was placed on improving the efficiency of anaerobic digester for POME treatment. However, intrinsic properties of POME (i.e., high content of fibrous materials, oil and solids) and its varying characteristics throughout the year have rendered the digestion process in producing effluent and biogas of consistent quality. To address these issues, alteration of characteristics for the anaerobic digestion feed stream would be helpful.

The proposed alteration substitution of cooling pond with thermal pretreatment coupled with a dewatering device (Khadaroo et al., 2019b). Khadaroo et al. (2019b) reported that thermal pretreatment helps to induce the breakdown of complex molecules in POME. Thermal pretreatment enhances the anaerobic digestion performance and improves dewaterability of POME. Furthermore, it does not require re-neutralization of effluent after treatment, as compared to the commonly used chemical pretreatment techniques (Khadaroo et al., 2019b).

A dewatering device (e.g., a thickener) permits the removal of impurities and microorganisms from POME and aids in solid–liquid separation process. The thickener enhances the anaerobic digester's performance by integrating a configuration

to control the load of the digesters since the physicochemical properties of POME are influenced by the efficiency of the oil extraction process along with high and low crop seasons (Poh & Chong, 2014). Different studies were conducted to observe the effect of dewatering and thermal pretreatment on the anaerobic digestion of POME (Khadaroo et al., 2020a). An energy analysis was also conducted to investigate the potential electricity generated from the proposed treatment process (Khadaroo et al., 2021).

3.1 Materials and Methods

3.1.1 Thermal Pretreatment and Dewatering

Raw POME was collected at the Sime Darby East Oil Mill, Malaysia. At the sampling location, the temperature of POME was measured to be 65 °C. The inoculum, anaerobic seed sludge was collected at the same mill. A total of 5 L of raw POME is placed in a beaker covered with aluminum foil and was thermally pretreated at 120 °C in an oven. The medium was stirred occasionally. The temperature was measured using an infrared thermometer at different heights along the beaker to ensure a uniform temperature.

After thermal pretreatment, the pretreated POME was placed in a settling column of 0.7 m height consisting of multiple sampling points to allow the removal of the different phases (oil, clarified liquid, and settled solids). The solid flocs in POME were allowed to settle for 24 h, at room condition. Samples of settled solids and clear liquid were extracted and hereafter denoted by "solid, S" and "liquid, L", respectively.

3.1.2 Anaerobic Digestion and Standard Methods for Parameters Testing

The chosen mode of anaerobic digestion was thermophilic batch anaerobic digestion. Once the different phases were extracted, they were recombined to make up the desired ratio. The sought ratio was poured in a 250 mL Schott bottle having two outlets. The operating volume was set at 100 mL. The inoculum volume was carefully selected and retained at 20% of the working volume during the course of the experiments. A reactor with a temperature of 55 °C under anaerobic conditions was used to cultivate and acclimatize the inoculum for 30 days to enable the bacteria consortium to be acclimatized to the conditions at which the anaerobic digestions experiments were conducted (Poh & Chong, 2014).

The inoculum volume was kept constant in all experimental runs for the evaluation of thermal pretreatment effects on anaerobic digestion performance of different solid: liquid ratios. A hot plate magnetic stirrer was used to heat the digesters and to ensure the medium for proper homogenization. The digesters were linked to a water displacement column using silicone tubes to facilitate the measurement of the

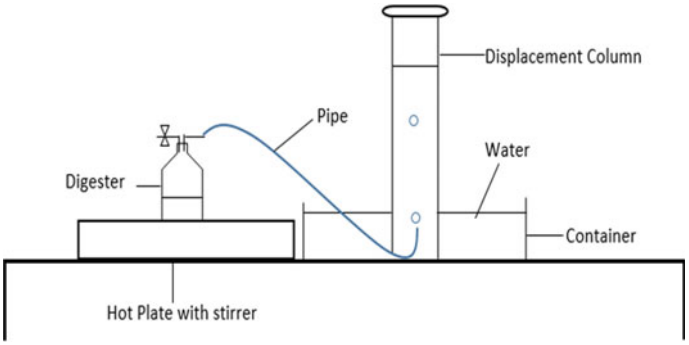

Fig. 5 Setup of thermophilic anaerobic digestion of POME

volume of the biogas generated as shown in Fig. 5. The pH of water was dosed to 2.0 using 1 M H_2SO_4 to avert the dissolution of carbon dioxide into the water, as per ASTM D5511 standard for the displacement column set up (Khadaroo et al., 2020b). This technique ascertains that the biogas mensuration using water displacement provides a more accurate result (Müller et al., 2004). The pH of the system was maintained between 6.8 and 8.0 by adjusting with 1 M $NaHCO_3$ to ensure optimum conditions. The pH was measured daily to assure that it lied within the mentioned range. The biogas composition in terms of methane, hydrogen sulfide, and carbon dioxide concentrations was evaluated using Binder COMBIMASS Gas Analyzer. The experiments were stopped when no more methane was measured in the digesters by Binder COMBIMASS Gas Analyzer (Khadaroo et al., 2020b).

3.2 Results and Discussion

Results presented in Fig. 6, Tables 4 and 5 show that thermally pretreated solid loadings in all tested conditions show increased biogas production, methane composition, as well as higher removal efficiencies of BOD, COD, TSS, and O&G. The best performing ratio was identified as 40 solid: 60 liquid (denoted as 40S:60L).

3.2.1 Biogas Generation and Methane Yield

The biogas production for the thermally pretreated 20S:80L POME reached 1470 mL which accounted for 960 mL more biogas than its untreated counterpart. The thermally treated 40S:60L POME produced 1886 mL of biogas, which is 456 and 415 mL more biogas in comparison to the untreated 40S:60L POME and the thermally pretreated 20S:80L POME, respectively.

The treated 50S:50L POME yielded 1509 mL biogas. The treated 50S:50L POME produced 187 mL more biogas than its untreated counterpart and 377 mL less biogas

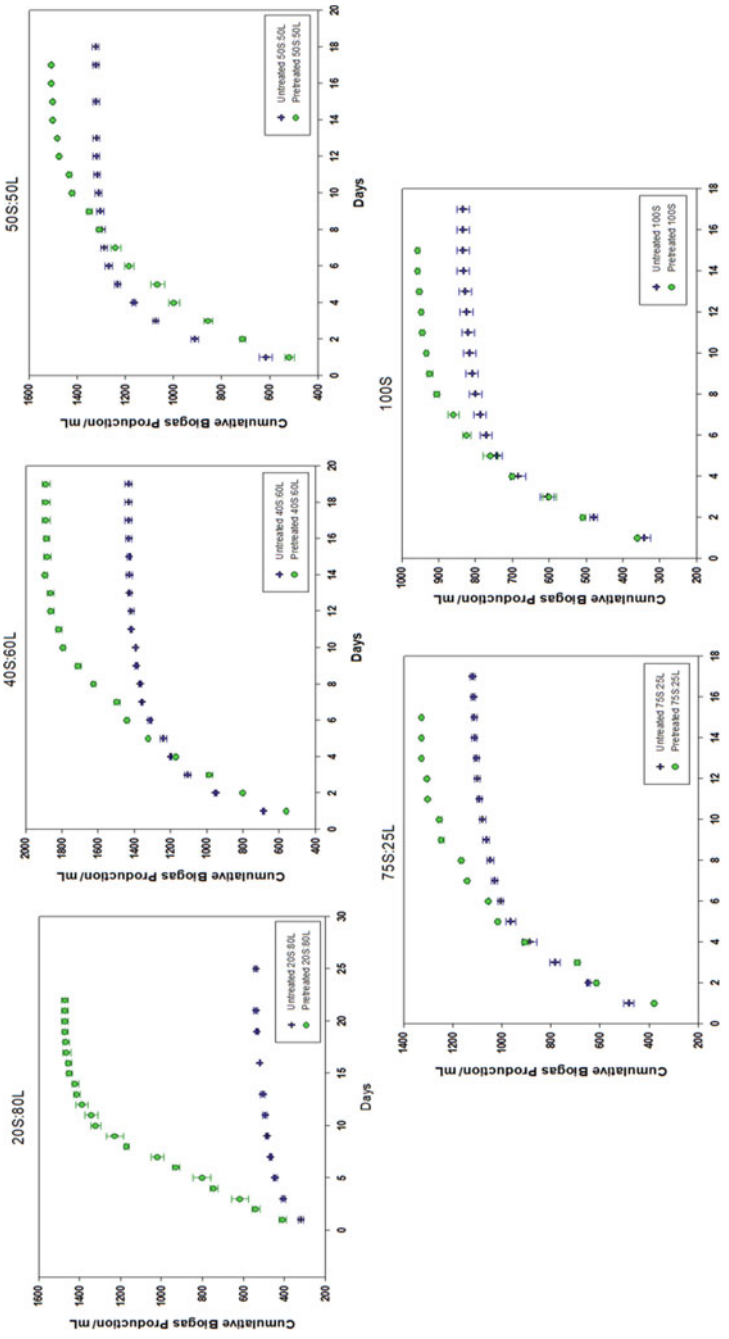

Fig. 6 Cumulative biogas production graphs of the thermally pretreated and untreated POME ratios (20S:80L, 40S:60L, 50S:50L, 75S:25L, 100S)

Table 4 Results obtained for the thermophilic anaerobic digestion of untreated POME at different solid loadings

Ratios	Dry solids content/%TS	Initial pH	Final pH	Cumulative biogas production/mL	Maximum methane composition /%	Minimum methane composition /%	H_2S composition/mg/L	Total anaerobes/100 mL	Duration of experiment /days	COD removal/%	BOD removal/%	TSS removal/%	O&G removal/%
20S:80L	3.29	7.23 ±0.05	7.52 ±0.03	539.44 ±10.29	73.83 ±2.42	50.36 ±2.07	204±4	1.2×10^6	≈25	62.53 ±1.14	58.07 ±1.76	55.44 ±3.46	26.20 ±0.46
40S:60L	4.02	7.21 ±0.02	7.74 ±0.09	1431.67 ±17.56	77.33 ±1.20	57.80 ±2.67	341±16	2.1×10^6	≈20	48.89 ±1.12	32.64 ±1.66	39.57 ±2.26	25.05 ±0.62
50S:50L	5.25	7.22 ±0.12	7.56 ±0.04	1322.78 ±13.62	64.26 ±2.71	54.13 ±0.87	560±21	7.5×10^5	≈18	33.26 ±0.71	23.97 ±1.30	29.40 ±1.55	19.24 ±0.45
75S:25L	6.4	7.27 ±0.10	7.44 ±0.04	1122.70 ±9.94	57.73 ±1.62	40.67 ±0.58	1823±23	1.5×10^5	≈17	23.11 ±0.41	24.10 ±0.52	20.76 ±0.57	26.57 ±0.18
100S	7.86	7.23 ±0.07	7.75 ±0.07	833.88 ±17.11	33.17 ±1.30	20.87 ±3.04	2968±52	9.3×10^4	≈17	7.67 ±1.05	21.78 ±1.84	19.06 ±2.85	31.16 ±0.62

Table 5 Results obtained for the thermophilic anaerobic digestion of thermally pretreated POME at different solid loadings

Ratios	Dry solids content/%TS	Initial pH	Final pH	Cumulative biogas production/mL	Maximum methane composition/%	Minimum methane composition/%	Total anaerobes/100 mL	Duration of experiment /days	COD removal/%	BOD removal/%	TSS removal/%	O&G removal/%
20S:80L	2.88	7.23 ±0.04	7.53 ±0.02	1471.10 ±15.23	79.23 ±1.34	71.30 ±2.71	1.5×10^6	≈ 22	84.50 ±1.01	84.41 ±0.15	83.03 ±0.91	82.88 ±0.34
40S:60L	3.98	7.27 ±0.02	7.57 ±0.07	1886.11 ±21.63	83.40 ±0.31	78.83 ±1.31	4.6×10^6	≈ 19	81.63 ±0.46	81.01 ±1.16	80.72 ±0.16	80.02 ±0.11
50S:50L	5.14	7.30 ±0.05	7.48 ±0.02	1509.43 ±4.43	76.97 ±0.73	71.40 ±0.79	1.1×10^6	≈ 17	65.38 ±0.04	62.72 ±0.36	67.20 ±0.75	64.81 ±0.40
75S:25L	6.32	7.20 ±0.02	7.71 ±0.06	1326.13 ±4.74	51.97 ±2.03	43.00 ±2.35	2.4×10^5	≈15	51.51 ±1.62	50.88 ±0.56	53.32 ±0.36	50.56 ±1.12
100S:0L	7.29	7.22 ±0.01	7.58 ±0.06	970.00 ±2.89	38.20 ±0.75	23.24 ±1.25	1.5×10^5	≈15	41.40 ±1.39	40.12 ±2.16	40.59 ±1.84	50.65 ±1.54

than the thermally treated 40S:60L solid loading. Similar observations could be found with the 75S:25L and 100S POME. Based on the results of the study, increasing the solid fraction of POME improved biogas production but up to 40% solids only. Meanwhile, the introduction of thermal pretreatment to POME is advantageous, as it improved the biogas yield as compared to the untreated POME.

The methane yield was computed to be 36.20 and 313.18 mL CH_4/g $COD_{removed}$ for the untreated and thermally treated 20S:80L solid loading. This accounted for a ninefold increase in the methane yield in the 20S:80L solid loading. The untreated and treated 40S:60L achieved a methane yield of 58.40 and 328.73mLCH_4/g$COD_{removed,}$ resulting in a sixfold increase in the methane yield. The 50S:50L solid loading attained a methane yield of 40.66 and 89.88mLCH_4/g$COD_{removed}$ for the untreated and treated counterparts, respectively, accounting for a twofold increase in the methane yield. The 75S:25L recorded a methane yield of 27.84 and 54.06 mLCH_4/g$COD_{removed}$, for the non-pretreated and thermally treated assays. The methane yield calculated for the untreated and treated 100S solid loading were 16.69 and 31.52mLCH_4/g$COD_{removed,}$ respectively. Both the treated 75S:25L and 100S had a twofold increase in the methane yield compared to their untreated counterparts. This further asserts the need for POME to undergo thermal pretreatment prior to anaerobic digestion.

3.2.2 Removal Efficiencies

The removal efficiencies of BOD, COD, TSS, and O&G were also investigated for all tested conditions. Post anaerobic digestion of the thermally treated 20S:80L POME, the COD, BOD, TSS, and O&G drastically decreased to 4696 ± 305, 1986 ± 150, 1866 ± 100, and 34 ± 1 mg/L resulting in a conspicuous percentage removal of 84.50 ± 1.01, 84.41 ± 0.15, 83.03 ± 0.91 and 82.88 ± 0.31% of COD, BOD, TSS, and O&G, respectively (Khadaroo et al., 2020b).

Before anaerobic digestion, the COD, BOD, TSS, and O&G of pretreated 40S:60L solid loading were measured as 40,800 ± 100, 20,090 ± 130, 16,000 ± 150, and 208 ± 12 mg/L. After anaerobic digestion, the COD, BOD, TSS, and O&G radically declined to 8155 ± 44, 4015 ± 67, 3162 ± 65, and 42 ± 1. These correspond to a remarkable removal percentage of 80.63 ± 0.46, 81.01 ± 1.16, 80.72 ± 0.16, and 80.02 ± 0.11% of COD, BOD, TSS, and O&G, respectively. The treated 40S:60L POME had a higher removal efficiency of 32.74, 48.37, 41.15, and 54.97% in terms of COD, BOD, TSS, and O&G congruently compared to the untreated 40S:60L assays (Khadaroo et al., 2020a). The above-mentioned results are summarized in Tables 4 and 5 where similar trends of biogas production were observed.

3.2.3 Energy Analysis for the Proposed Treatment System

Assuming that a medium-capacity plant treats 567.4 m^3 of POME per day (Sarwani et al., 2019). Electricity consumed in thermophilic anaerobic digestion and thermal

pretreatment was evaluated to be 1.61 × 104 and 1.53 × 104 kWh/d, congruently. These values were determined by upscaling the results obtained from laboratory-scale experiments.

Some assumptions made for the energy analysis calculations. Firstly, no heat is lost to the environment. Secondly, there is only very insignificant (if any) transfer of energy to the walls of the tank, since the latter was further insulated. Finally, it was presumed that the specific heat capacity is similar to that of water which is 4.18 J/g °C (The density of POME was measured to be equal to that of water (Khadaroo et al., 2019a)).

In Table 6, it can be noted that thermophilic anaerobic digestion is able to bring forth nearly three times more electricity compared to the existing process. Meanwhile, the proposed treatment process consisting of the integration of thermal pretreatment and dewatering with an optimum 40S:60L solid loading achieved a total electricity generation of 75-fold greater compared to the existing treatment. Then again, the treated 50S:50L solid loading generated 14.6 times more electricity than that of the current treatment process. The high electricity generation is due to a higher volume of biogas produced with a superior methane purity compared to the 50S:50L solid loading and the other testes conditions. When extrapolating to an industrial scale, the outcome can be considerable concerning electricity generation. The findings above proved that the integration of thermal pretreatment and dewatering can substantially improve POME's treatment process while making the process more sustainable.

4 Post-Treatment of Anaerobically Treated POME with Assisted Microbubble Flotation

While the limitations of anaerobic digestion of POME could be solved via automation of anaerobic digester, adoption of thermal pretreatment, and dewatering processes, the effluent produced from anaerobic digestion still does not meet the regulatory standards. Therefore, it is essential to identify a treatment process that could replace the facultative ponds which have long treatment periods and occupy a large space in the palm oil mill. In this study, microbubble flotation was as a method to post-treat the anaerobic digested POME and the sub-sections below describe the methodology and the results of the study.

Table 6 Energy analysis case study on a medium-capacity plant

	Mesophilic AD without pretreatment (Sarwani et al., 2019)	Thermophilic AD without pretreatment (Khadaroo et al., 2021)	Thermophilic AD with pretreated 40S:60L (Khadaroo et al., 2021)	Thermophilic AD with pretreated 50S:50L (Khadaroo et al., 2021)
Biogas produced/m^3/d	28.36	2.61×10^3	5.45×10^3	4.53×10^3
Percentage CH_4 in biogas/%	55.0	61.9	77.8	72.5
CH_4 produced/m^3/d	15.6	1.62×10^3	4.24×10^3	3.29×10^3
Energy produced from CH_4/kJ/d	5.78×10^5	5.98×10^7	1.57×10^8	1.22×10^8
Electricity generated/kWh/d	1.60×10^2	1.66×10^4	4.35×10^4	3.38×10^4
Electricity consumed/kWh/d	–	1.61×10^4	3.15×10^4	3.15×10^4
Extra electricity generated/kWh/d	–	4.71×10^2	1.21×10^4	2.34×10^3
Extra electricity generated compared to conventional process/fold	–	2.9	75.1	14.6

4.1 Materials and Methods

4.1.1 Imaging and the Bubble Treatment of Anaerobically Treated POME

Figure 7 depicts the experimental setup for the microbubble flotation rig. The experimental setup consisted of a centrifugal pump (LangYou, LYQB-60, 370 W), microbubble generator (venturi), and two ball valves. In the flotation chamber, the water was continuously pumped from the lowermost section of the column using the venturi system. Air was drawn and inserted into the column, which created pressure difference between the inlet and throat of the venturi. The chosen flow rate of water was 0.331 and 0.44 L/s. A bubble generating device was integrated at the bottom of the column. Sampling was undertaken using a syringe which was coupled to a tube, in which water was drawn out from the midsection of the column. All experiments were undertaken in batches with a working volume of 1.5L.

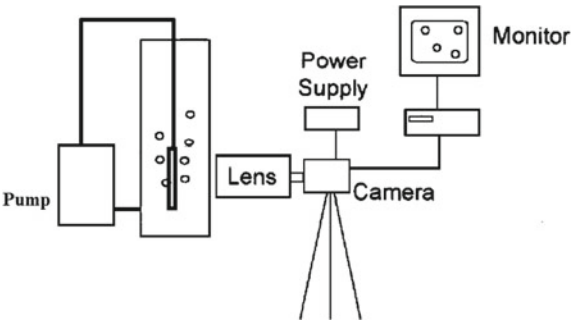

Fig. 7 Charge-coupled device (CCD) setup to capture the microbubble

4.1.2 Jar Test

Poly-aluminum chloride (PAC) coagulant of 30% concentration in white powder form was used in the experiments. After bubbling, the anaerobically treated POME was kept and utilized to undertake the jar test. The coagulation-flocculation examination was conducted using the traditional jar apparatus (VELP Scientifica Flocculator, JLT4). A 4-steel spindless paddle flocculator was utilized to stir the medium at a uniform speed. A 300 mL volume of 2.22 times diluted POME was placed in each beaker. Various concentrations of PAC coagulant ranging from a concentration of 0.5–6 g/L were used. The medium was mixed at a steady mixing rate of 150 rpm for a duration of five min. The setup was then altered to provide a slower mixing speed of 10 rpm with the steel paddle lifted halfway up the beaker to ameliorate the formation of flocs. The jar test was undertaken at a temperature of 25 °C. The sedimentation time was set to 30 min and supernatant of the treated POME was collected for further analysis.

4.2 Results and Discussion

4.2.1 COD (Chemical Oxygen Demand)

After multiple trials, it was observed that a minimum flow within the pump was required to prevent axial load on the pump shaft to be surpassed. Table 7 indicates the pH recorded prior to and post microbubble flotation for medium and high flow rates using the anaerobically treated POME. After microbubble flotation, the pH of the effluent was observed to increase ranging from 7.33 to 8.07. Table 7 shows that, after treatment, the pH of effluent increases with extended bubbling duration. However, in Fig. 8, it can be observed that at pH less than 8, the COD removal efficiency declined. An explanation for the latter is that the generation of bubbles between pH 7–8 tends to exhibit low negative zeta potential. Microbubbles with low charge cannot efficiently get rid of suspended solids in the wastewater. Furthermore, oxidation owing to the rupture of microbubbles tends to form hydroxyl radicals. The

adherence of suspended matter to the low-charged microbubbles promotes to the removal of organic matter within the wastewater.

From Fig. 8, it can be seen that when the bubbling time was prolonged from 2.5 to 12.5 min, the COD removal efficiency increased from 9.8 to 53.7% and from 14 to 45.9% for bubbles of sizes 469 and 379.92 μm, congruently. In comparison to the bubbles generated at two different flow rates, $D_{32} = 379.92$ μm with smaller diameter showed a higher COD removal rate for bubbling time of 2.5–10 min. The latter occurs since the smaller bubbles accelerate the hydroxyl radical's formation due to elevated inner pressure which can break the conjugated carbon–carbon double bonds in melanoidins. The melanoidins are accountable for POME's brown color. In another study, it was stated that hydroxyl radicals produced in a small amount promote the breakdown of the organic matter present in the wastewater (Liu, et al., 2012).

Table 7 pH and temperature reading for different bubbling time

Parameters [a]	Anaerobically digested POME (ADPOME)	Effluent after microbubble flotation (19.8 L/min)	Effluent after microbubble flotation (26.4 L/min)	Effluent after microbubble flotation (19.8 L/min) + PAC coagulation	DOE discharge standard
pH	7.05	8.06	8.07	6.28	5–9
Temperature	18	26	27	25	45
COD	21,025	9725	11,375	1407	–
BOD	2220	510	1065	Not detected	100
TSS	17,995	7685	10,080	22	–
O&G	235	60	120	Not detected	50

[a]All units measured in mg/L except pH and temperature (°C)

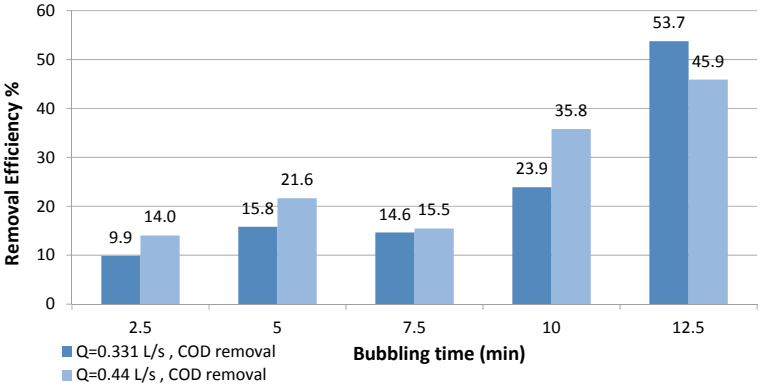

Fig. 8 Plot of COD removal at different bubbling times for $Q_L = 0.331$ L/s and $Q_L = 0.44$ L/s

Color change was observed at minutes 10 and 12.5 bubbling time; this occurred due to the hydroxyl radicals generated chemical reactions as the microbubbles are removed from the system. In general, smaller bubbles have a larger surface area. This is demonstrated in Eq. 5 for the relationship between surface area (S) and volume (V).

$$\frac{s}{v} = \frac{4\pi r^2}{4/3\pi r^3} = \frac{3}{r} \tag{5}$$

Small bubbles have larger surface area, which enhances bubble-particles collision efficiency and resulting in an augmented COD removal efficiency. Nonetheless, as bubbling time was extended, bubbles of size $D_{32} = 469$ μm were noted to achieve a superior removal rate with a highest COD removal of 53.7%. It was determined that floated microbubbles tend to produce a foam that cannot be broken down easily. It was observed when the water was recirculated at a higher flow rate, a larger amount of foam was brought forth. Due to foaming, the water level in the column decreased substantially, making shorter distances accessible for the bubbles. This phenomenon indicated that at higher flow rates, the generation of smaller bubbles with larger surface areas lessened the displacement room for the bubble to move owing to the generation of a large amount of foam. Subsequently, the possibility of contact between the bubble and the contaminants in the medium is therefore drastically reduced. Hence, COD removal rate decreases when bigger bubbles are used.

4.2.2 BOD (Biochemical Oxygen Demand)

The BOD removal rate was observed to progressively increase with bubbling time, ranging from 51.8 to 77% for $D_{32} = 469$ μm and 29.7 to 52% for $D_{32} = 379.92$ μm. The trend indicates that a prolonged bubbling time will enhance the BOD removal efficiency. Nonetheless, the latter was not observed for higher flow rates generated microbubbles. Figure 9 shows the BOD removal efficiency of this method.

It was deduced upon those smaller microbubbles having larger total surface areas, would impart higher flotation efficiency of particles in a fluid body owing to a more elevated flux in mass transfer. However, the opposite was observed in the BOD removal trend. In turn, it was noted that smaller microbubbles (0.44 L/s) attained lesser removal efficiency. It can therefore be hypothesized that the influence of surface area on the removal efficiency took precedence over the impact of rising velocity. An explanation for this is that more particles are attracted to smaller bubble sizes, however, low rising velocity allows less bubbles to reach the surface in the set period of time. The latter causes the removal rate to decrease. This phenomenon is especially conspicuous due to the presence of large complex organic masses, resulting in a further curbed rising velocity and BOD removal efficiency.

The BOD parameter primarily relates to the concentration of organic particles in the POME colloid while the COD pertains to the conglomerate concentrations

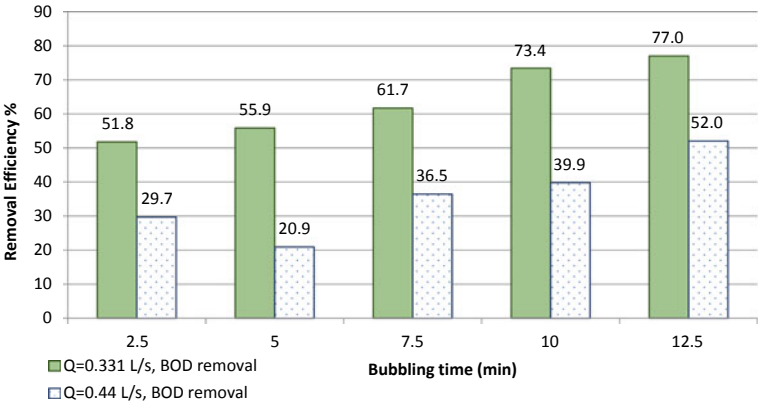

Fig. 9 Plot of BOD removal at different bubbling times for $Q_L = 0.331$ L/s and $Q_L = 0.44$ L/s

of both inorganic and organic molecules. From the results, it was found that the bubbling treatment yielded higher BOD removal efficiency compared to the COD removal rate, indicating that micro bubbling flotation treatment is more efficient in degrading organic particles than inorganic particles (Nguyen & Evans, 2004).

4.2.3 Oil and Grease (O&G)

Figure 10 shows the results obtained for the removal efficiency of O&G insoluble organic compounds in POME. It can be noted that as increasing bubbling time enhanced O&G removal efficiency. The removal efficiencies of microbubbles with bubble diameter of $D_{32} = 469$ μm and $D_{32} = 379.92$ μm were found to be 10.6% to 74.5% and 3% to 48.9%, respectively. From the study, it was noted that as increased temperature and pH enhanced the removal of oil. The latter can be explained by the influence of several physicochemical characteristics of oil and grease content in POME (Ahmad et al., 2003). The rise in temperature occurs due to cavitation and friction of the pump. While the increase in pH is related to the dissociation of OH^- ions in water, spurring the OH^- ions to react with residual oil bringing forth saponification. The latter produced soap that is soluble in water, resulting in a larger O&G removal efficiency at prolonged bubbling times (Ahmad et al., 2003).

Ahmad et al. (2003) reported that at pH levels greater than 7, oil compounds display a higher chemical attraction (affinity) for negatively charged surfaces. The oil droplets are attracted to negative ions which give rise to negatively charged particles (Ghernaout & Ghernaout, 2012). The latter is a potential explanation for the elevated O&G removal efficiency depicted in Fig. 9 with extended bubbling time. It is therefore sensible to conclude that adsorption on the surface of the bubbles is more conducive as bubbling time is extended.

When comparing the 10 and 12.5 min bubbling times in Fig. 10, treated POME with a bubble of size 469 μm resulted in a higher O&G removal efficiency. The

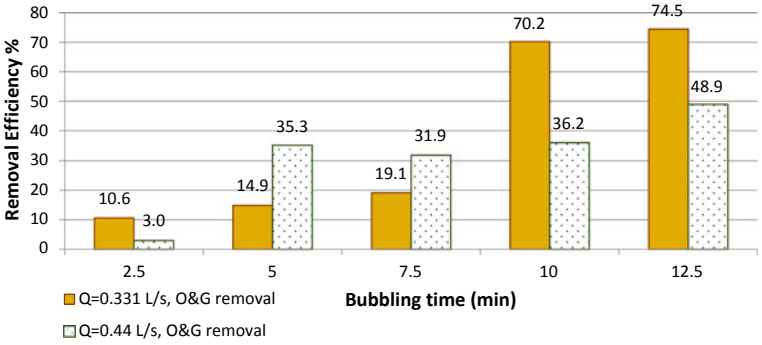

Fig. 10 Plot of O&G removal at different bubbling times for $Q_L = 0.331$ L/s and $Q_L = 0.44$ L/s

smaller bubbles with larger surface areas (at a higher flow rate) had a lower O&G removal rate, as compared to larger microbubbles when the bubbling time was increased. The smaller-sized microbubbles attained a lower O&G removal rate since low rising velocity was prevailing as a fundamental parameter in removal efficiency in comparison to the total surface area. The latter can be explained by the long carbon chains found in oil and grease molecules; thus, the molecular masses tend to be heavier. Therefore, bigger microbubbles with greater rising velocity can float and adhere to the heavy oil particles, efficiently removing the latter.

5 Conclusion

The advancement in technologies available for the treatment of POME has rapidly evolved over the years owing to the intrinsic challenges surrounding the treatment process of POME, the fluctuating characteristics of POME, the lack of skilled labor to manage the treatment process as well as more stringent regulations when it comes to the discharge of the latter. Solutions employed to mitigate the aforementioned predicaments must be efficient, technically, economically, and environmentally feasible. In other words, the technology has to be practically and efficiently utilized in the mills. Besides, it has to be economically viable and environmental-friendly. This can be achieved through the reduction in greenhouse gases emission and treated effluent that meets the environmental standards. The introduction of an "artificial brain", thermal pretreatment coupled with a dewatering device, and coagulant-aided microbubble flotation for POME treatment process enhance the treatment efficacy and increase biogas generation. In the future, pilot-scale studies which incorporate all three aspects mentioned above will be carried out in collaboration with palm oil mill practitioners to ensure effective implementation of these technologies, in order to enhance the POME treatment processes.

References

Ahmad, A., Ismail, S., Ibrahim, N., & Bhatia, S. (2003). Removal of suspended solids and residual oil from palm oil mill effluent. *Journal of Chemical Technology and Biotechnology, 78*, 971–978.

Chin, M. J., Poh, P. E., Tey, B. T., Chan, E. S., & Chin, K. L. (2013). Biogas from palm oil mill effluent (POME): Opportunities and challenges from Malaysia's perspective. *Renewable and Sustainable Energy Reviews, 26*, 717–726.

Ghernaout, D., & Ghernaout, B. (2012). Sweep flocculation as a second form of charge neutralization—A review. *Desalination and Water Treatment, 3*(44), 15–28.

Hamawand, I., & Baillie, C. (2015). Anaerobic digestion and biogas potential: Simulation of lab and industrial-scale processes. *Energies, 8*, 454–474.

Khadaroo, S. N. B. A. (2021). *Integration of thermal pretreatment and dewatering in the anaerobic co-digestion of palm oil mill effluent (POME) for enhanced treatment performance in terms of biogas production and treated effluent quality*. Monash University.

Khadaroo, S. N. B. A., Poh, P. E., Gouwanda, D., & Grassia, P. (2019b). Applicability of various pretreatment techniques to enhance the anaerobic digestion of palm oil mill effluent (POME): A review. *Journal of Environmental Chemical Engineering, 7*, 103310. https://doi.org/10.1016/j.jece.2019.103310

Khadaroo, S. N. B. A., Grassia, P., Gouwanda, D., & Poh, P. E. (2020a). The impact of thermal pretreatment on various solid-liquid ratios of palm oil mill effluent (POME) for enhanced thermophilic anaerobic digestion performance. *Journal of Cleaner Production, 261*, 121159. https://doi.org/10.1016/j.jclepro.2020.121159

Khadaroo, S. N. B. A., Grassia, P., Gouwanda, D., & Poh, P. E. (2019a). Is the dewatering of palm oil mill effluent (POME) feasible? Effect of temperature on POME's rheological properties and compressive behavior. *Chemical Engineering Science, 202*, 519–528. https://doi.org/10.1016/j.ces.2019.03.051

Khadaroo, S. N. B. A., Grassia, P., Gouwanda, D., & Poh, P. E. (2020b). The influence of different solid-liquid ratios on the thermophilic anaerobic digestion performance of palm oil mill effluent (POME). *Journal of Environmental Management, 257*, 109996. https://doi.org/10.1016/j.jenvman.2019.109996

Liu, S., et al. (2012). The effect of different types of micro-bubbles on the performance of the coagulation flotation process for coke waste-water. *Journal of Chemical Technology & Biotechnology, 87*, 206–215.

Menon, N. R. (2011). Development of palm oil mill technology. *Palm Oil Engineering Bulletin, 100*, 39–53.

Moreno PA (2004). Evaluation of factors responsible for high effluent suspended solids events in the Kuwahee wastewater treatment plant. Masters Theses. University of Tennessee, Knoxville "Trace: Tennessee Research and Creative Exchange".

Murphy, S., 2007. General information on solids. *City of Boulder/ USGS Water Quality Monitoring*. http://bcn.boulder.co.us/basin/data/BACT/info/TSS.html

Müller, W. R., Frommert, I., & Jörg, R. (2004). Standardized methods for anaerobic biodegradability testing. *Re/Views in Environmental Science & Bio/Technology*, 3(2), 141–158. https://doi.org/10.1007/s11157-004-4350-6

Nguyen, A., & Evans, G. (2004). Attachment interaction between air bubbles and particles in froth flotation. *Experimental Thermal and Fluid Science, 28*(5), 381–385.

Poh, P. E., & Chong, M. F. (2014). Upflow anaerobic sludge blanket-hollow centered packed bed (UASB-HCPB) reactor for thermophilic palm oil mill effluent (POME) treatment. *Biomass and Bioenergy, 67*, 231–242. https://doi.org/10.1016/j.biombioe.2014.05.007

Poh, P. E., Yong, W. J., & Chong, M. F. (2010). Palm oil mill effluent (POME) characteristic in high crop season and the applicability of high-rate anaerobic bioreactors for the treatment of POME. *Industrial & Engineering Chemistry Research, 49*(22), 11732-11740. https://doi.org/10.1021/ie101486w

Poh, P. E, Khadaroo, Sabeeha. N. B. A, Tan, H. M., & Gouwanda, D. (2020). An official publication of the Malaysian Palm Oil Council (MPOC) advancing on palm oil mill effluent (POME) treatment—What is in store for you? *Journal of Oil Palm, Environment & Health, 11*, 6–12. https://doi.org/10.5366/jope.2020.02

Sarwani, M. K. I., Fawzi, M., Osman, S. A., & Nasrin, A. B. (2019). Bio-methane from palm oil mill effluent (POME): Transportation fuel potential in Malaysia. *Journal of Advanced Research in Fluid Mechanics and Thermal Sciences, 1*, 1–11.

Tan, H. M., Gouwanda, D., & Poh, P. E. (2018a). Adaptive neural-fuzzy inference system versus anaerobic digestion model No.1 for performance prediction of thermophilic anaerobic digestion of palm oil mill effluent. *Process Safety and Environment Protection, 117*, 92–99. https://doi.org/10.1016/j.psep.2018.04.013

Tan, H. M., Poh, P. E., & Gouwanda, D. (2018b). Resolving stability issue of thermophilic high-rate anaerobic palm oil mill effluent treatment via adaptive neuro-fuzzy inference system predictive model. *Journal of Cleaner Production, 198*, 797–805. https://doi.org/10.1016/j.jclepro.2018.07.027

Zhao, L., Dai, T., Qiao, Z., Sun, P., Hao, J., & Yang, Y. (2020). Application of artificial intelligence to wastewater treatment: a bibliometric analysis and systematic review of technology, economy, management, and wastewater reuse. *Process Safety and Environmental Protection, 133*, 169–182. https://doi.org/10.1016/j.psep.2019.11.014